NANO LETTERS

2001
Vol. 1, No. 7
353−359

Photodimerization of Cinnamate Derivatives Studied by STM

Mohamed M. S. Abdel-Mottaleb,[†] Steven De Feyter,*[,†] Andre Gesquière,[†] Michel Sieffert,[‡] Markus Klapper,[‡] Klaus Müllen,[‡] and Frans C. De Schryver*[,†]

Department of Chemistry, Laboratory of Molecular Dynamics and Spectroscopy, University of Leuven (KULeuven), Celestijnenlaan 200-F, 3001 Heverlee, Belgium, and Max-Planck Institute for Polymer Research, Ackermannweg 10, D-55128 Mainz, Germany

Received May 23, 2001

Ⓦ This paper contains enhanced objects available on the Internet at http://pubs.acs.org/nano.

ABSTRACT

The photochemical dimerization of two cinnamate derivatives, C18CinnC18 and C18CinnC10, has been investigated at the liquid/graphite interface by scanning tunneling microscopy (STM). The unit cell parameters of the two derivatives as deduced from the STM images indicate that the photodimerization reaction should not occur according to the topochemical postulates. Nevertheless, C18CinnC18 does photodimerize upon irradiation of its monolayer, while C18CinnC10 does not.

Self-assembled monolayers of a wide range of organic compounds have been studied with scanning tunneling microscopy (STM) at the graphite/liquid interface.[1−5] These monolayers, which are formed by physisorption of molecules from solution on solid substrates, have been visualized with submolecular resolution. In these kind of systems, STM allows not only for the study of the molecular organization in the monolayer, but also for the study of dynamic[6−8] and chemical[9−13] phenomena within the monolayer and between the monolayer and the liquid layer (supernatant solution) on top of the monolayer.

Reactivity of organic compounds at the graphite/liquid interface has been investigated for several systems using STM. In the majority of these reports, the reactions are photoinduced. Heinz et al. have reported on the phototransformation of 10-diazo-2-hexadecylanthrone to 2-hexadecyl-9,10-anthraquinone.[11] They were able to identify the reactant and the product at the graphite/liquid interface. Vanoppen et al. have reported the cis−trans isomerization of azobenzene derivatives. Domains of reagent and product of this reversible photoinduced reaction have been simultaneously imaged with submolecular resolution and identified at the graphite/liquid interface.[12] In all of these examples, the phototransformation occurred in the liquid phase on top of the graphite substrate. Only few systems have been reported where with absolute certainty photoinduced reactions at the liquid/graphite interface proceed only in the monolayer and not in the supernatant solution. For instance, Grim et al. have reported the photopolymerization of diacetylene molecules at the graphite/liquid interface.[13]

[2+2] Photodimerization reactions of cinnamic acid derivatives have been investigated extensively in three dimensions (3D). The classic studies by Schmidt et al. have demonstrated that the packing of molecules in the crystals "strictly" controls such reactions.[14−17] Some of these cinnamic acids dimerize upon irradiation with UV light, while in solution trans−cis isomerization occurs but not dimerization (Scheme 1). On the basis of extensive crystallographic and photochemical studies on cinnamic acids, Schmidt et al. drew the following conclusions: (a) the nature of the crystal structure determines whether the reaction can occur and also determines the molecular structures of the products, if any; (b) the reaction involves the combination between nearest neighbor molecules in a stack, and occurs with a minimum of atomic and molecular movement. A reaction that behaves in this way is said to be topochemically controlled.[14] These postulates imply that the reactive centers must be properly placed in the crystal for the reaction to occur, and that the topochemical processes are constrained by lattice forces that are assumed to maintain electronically excited molecules in structures close to the ones they adopted in their ground state. Cinnamic acid and its derivatives were observed to crystallize in three polymorphic forms and show photochemical behavior that is determined by this structure

* Corresponding authors. Tel: +32 (016) 32 74 05; Fax: +32 (016) 32 79 89. E-mail: Frans.DeSchryver@chem.kuleuven.ac.be; Steven.DeFeyter@chem.kuleuven.ac.be.
[†] University of Leuven (KULeuven).
[‡] Max-Planck Institute for Polymer Research.

10.1021/nl010034k CCC: $20.00
Published on Web 07/11/2001

Scheme 1. Reaction Products of the Different Packing Patterns of Cinnamic Acid Crystals upon Irradiation[a]

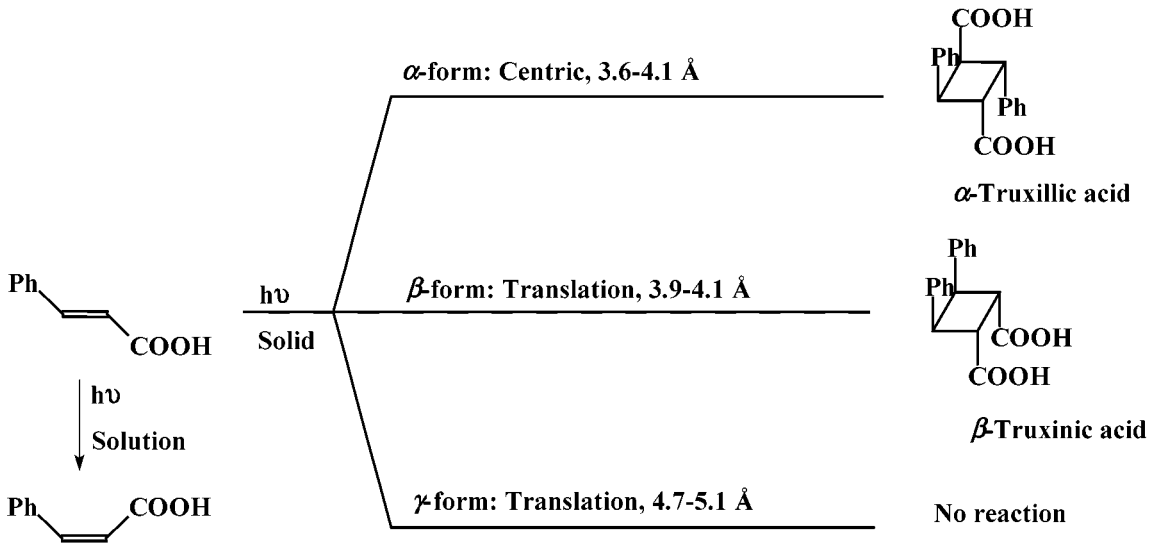

[a] The different crystal polymorphs, along with the symmetry relation and distance between reactive molecules are indicated.

type. The three structural types, namely α, β, and γ, differ in the distance between equivalent points of neighboring molecules, which is ~4.2 Å (centric double bond distance), 3.8−4.2 Å, and 4.8−5.2 Å, respectively.[14]

These topochemical postulates are landmarks in organic solid state photochemistry and are used as rules, as they are able to provide an understanding of a large number of [2+2] photodimerization reactions of widely varying structures.[17,18] However several examples do exist where the systems under investigation deviate significantly from the topochemical postulates suggested by Schmidt.[14−17] In some cases the distance between the interacting double bonds is larger than the proposed upper limit for interaction (4.2 Å) or the double bonds are not exactly parallel and yet the molecules photodimerize.[16−18] Two approaches have been used to explain the deviations from the topochemical postulates, namely "reaction cavity" and "dynamic preformation".[18]

In this paper, STM was used to investigate the two-dimensional (2D) organization and photodimerization of cinnamic acid derivatives at the graphite/liquid interface. The photoreactivity of a symmetrically substituted and an asymmetrically substituted cinnamic acid derivative was investigated. The difference in substitution is reflected in the 2D ordering and consequently also in the photoreactivity. The symmetric system was found to undergo photodimerization, despite the large distance between the adjacent double bonds. On the other hand, the asymmetric system is photostable. There is evidence for packing fluctuations in the monolayer, without which the reaction is not likely to proceed.

Prior to imaging, **trans-C18CinnC18** and **trans-C18-CinnC10** (Figure 1), of which the synthesis is given in the Supporting Information, were dissolved in 1-octanol (Aldrich, 99%) and a drop of either solution was applied on a freshly cleaved surface of highly oriented pyrolytic graphite (HOPG). The presented STM images were acquired in the variable current mode (constant height) under ambient conditions. In the STM images, white corresponds to the highest and black

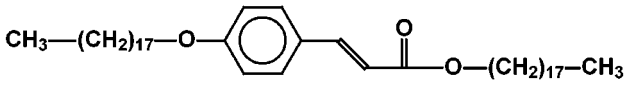

C18CinnC18

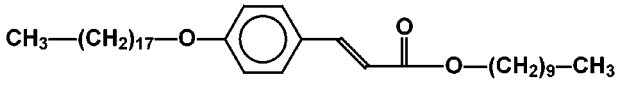

C18CinnC10

Figure 1. Chemical structure of **C18CinnC18** and **C18CinnC10**.

to the lowest measured tunneling current. STM experiments were performed using a Discoverer scanning tunneling microscope (Topometrix Inc., Santa Barbara, CA) with a typical frame acquisition time of 7 s, along with an external pulse/function generator (model HP 8111 A), with negative sample bias. Tips were etched electrochemically from Pt/Ir wire (80%/20%, diameter 0.2 mm) in a 2 N KOH/6 N NaCN solution in water. The experiments were repeated in several sessions using different tips to check for reproducibility and to avoid artifacts. Note that during the experiments, the STM tip is immersed in the supernatant solution. Different settings for the tunneling current and the bias voltage were used, ranging from 0.6 nA to 1 nA and −10 mV to −1.5 V, respectively. All STM images contain raw data and are not subjected to any manipulation or image processing.

When a drop of the solution of **C18CinnC18** in 1-octanol is applied to a freshly cleaved graphite surface, a physisorbed monolayer is spontaneously formed at the graphite/1-octanol interface. Figure 2a shows an image of such a monolayer observed with STM. The image is submolecularly resolved, which enables us to identify the cinnamate groups as well as the aliphatic chains. The brighter regions (higher tunneling current) in the STM image originate from the cinnamate moieties (indicated by a red arrow). The lamella is defined by two black troughs, which are characteristic for terminal

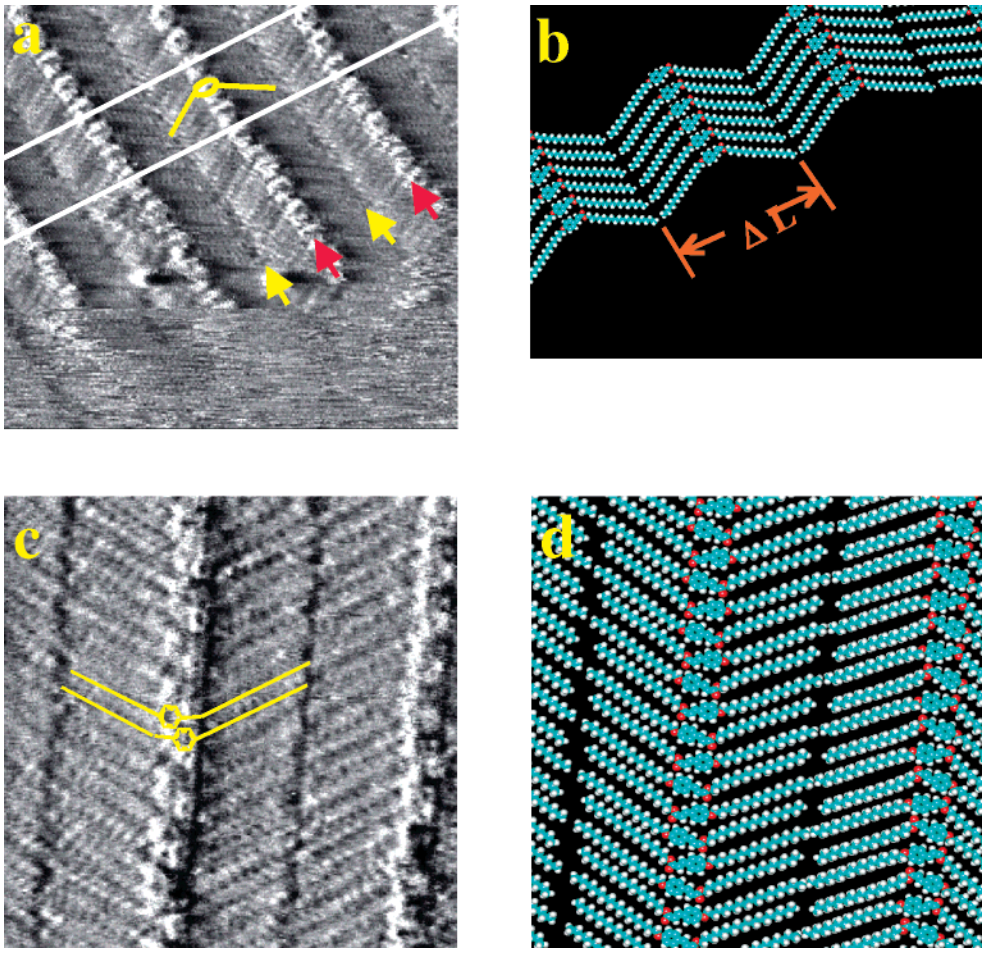

Figure 2. (a) STM image showing a Type 1 monolayer of **C18CinnC18** physisorbed at the graphite/liquid interface. Red arrows point to the cinnamate groups, yellow arrows define the lamella boundaries. One molecule is schematically drawn. The image area is 16 × 16 nm^2, $V_{set} = -0.312$ V, $I_{set} = 1.0$ nA. (b) Molecular model of the outlined area in a where $\Delta L = 54 \pm 3$ Å and $a = 6.3 \pm 0.5$ Å. (c) STM image showing a Type 2 monolayer of **C18CinnC18**. Two molecules are schematically drawn. The aryl moieties are clearly discerned; they are ordered in a zigzag orientation. The image area is 12 × 12 nm^2, $V_{set} = -0.48$ V, $I_{set} = 0.7$ nA. (d) Molecular model of the monolayer packing shown in c.

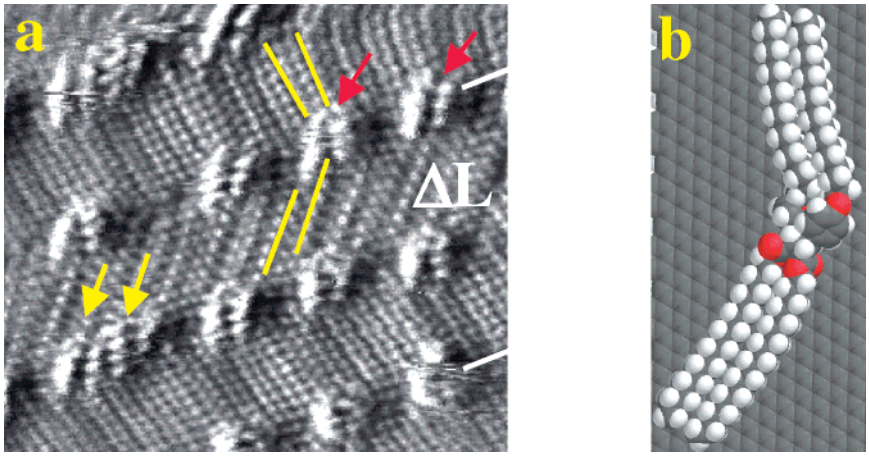

Figure 3. (a) STM image of the dimer. The U-shaped bright structures are correlated with the core of the dimer molecule (red arrows). To each bright structure four alkyl chains are connected (yellow lines). Image area is 10.7 × 10.7 nm^2, $V_{set} = -0.42$ V, $I_{set} = 0.7$ nA. (b) Molecular model showing a dimer molecule on the surface of graphite after geometry optimization by molecular mechanics calculations.

methyl groups (indicated by the two yellow arrows). From the STM image, the V-shape conformation of the molecule is clearly evident. To guide the eye, one **C18CinnC18** molecule has been drawn schematically in the STM image. Based upon the contrast of the cinnamate groups in this image it is obvious that the phenyl rings are aligned in a row. So all molecules are equivalent along the lamella axis. A molecular model for the observed packing is shown in

Figure 2b. The distance between two neighboring molecules within a lamella (a) is 6.3 ± 0.5 Å, the lamella width (ΔL) is 54 ± 3 Å, and the alkyl chains form an angle of 118 ± 4° with respect to the lamella axis as shown. These molecules do not form a true 2D crystal lattice, but rather parallel one-dimensional (1D) rows. The contrast of the cinnamate groups in some images, such as in Figure 2c, indicates that **C18CinnC18** can also arrange in a different way within the lamella. The STM image is of high resolution, individual aryl groups can clearly be discerned. The molecules in Figure 2a are packed in a way that the aryl groups in a given lamella are all lying along the same line (Type 1). On the other hand, close inspection of the STM image in Figure 2c reveals that the aryl groups in any given lamella are adopting a zigzag order (Type 2). Two molecules have been schematically drawn in the STM image. A molecular model representing the ordering of the molecules observed in this STM image is given in Figure 2d. The packing parameters of Type 2 do not differ from those of Type 1, within experimental error. The Type 2 orientation is not abundant but was imaged several times in different sessions.

To induce in-situ photodimerization of **C18CinnC18**, a UV lamp (CAMAG universal lamp, wavelength 300 nm) was used. Irradiation was carried out for different time intervals, which varied between 5 min and 5 days.[19] Images observed after illumination for more than 10 min showed a new packing pattern (Figure 3a). To each bright structure (core, indicated by red arrows) four alkyl chains (indicated by the yellow lines) are connected. Based upon the STM contrast, it can be concluded that the alkyl chains adopt two different orientations. The plane formed by the carbon backbone of alkyl chains on one side of the core lies perpendicular to the surface, while the carbon backbone of the alkyl chains on the other side of the core lies parallel to the surface.[20] At the left-bottom side of the image in Figure 3a, a change in the packing pattern of the adlayer can be observed. Two molecules are lying next to each other (the two molecules are pointed out with yellow arrows). Due to the change in the packing of the molecules in this lamella, there is a corresponding change in the neighboring lamella. The longer the irradiation time, the more of this new adlayer structure is observed. To understand the nature of the change in the packing pattern upon irradiation, solid crystals of **C18CinnC18** were irradiated at 300 nm up to 5 days and then dissolved in 1-octanol. Upon application of this solution to the graphite surface, the same features as observed in the STM image in Figure 3a are observed. Mass spectrometry showed the presence of dimers. These data strongly suggest that the new packing pattern is that of dimer adlayers. Upon ex-situ irradiation of highly diluted solutions ($\leq 10^{-6}$ M) of **C18CinnC18**, no evidence of dimer formation was detected by either STM or by other techniques (mass spectrometry). On the other hand, ex-situ irradiation of more concentrated solutions ($\geq 10^{-5}$ M) resulted in dimer formation. This was attributed to the formation of microcrystals. This suggests that upon in-situ irradiation of low concentrated solutions, the photodimerization of **C18CinnC18** occurs at the liquid/graphite interface.

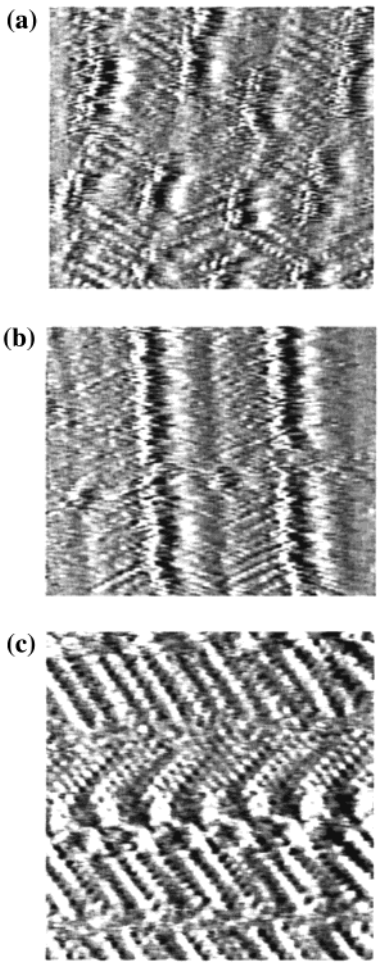

Figure 4. Still images representing movies 1, 2, and 3. (a) Movie 1 shows the dynamics of dimer formation at a monomer/dimer domain boundary. The distance between two cinnamate groups in a monomer domain measured perpendicular to the lamella axis is approximately twice that of the core-to-core distance in a dimer domain. This difference allows us to distinguish monomer and dimer domains and follow changes upon dimerization. In this movie, monomers can easily be identified in the upper part of the movie, while dimers are found in the lower part. During the imaging, the sample was illuminated (300 nm). At the monomer/dimer domain boundary, photodimerization of monomers causes changes in the packing in the upper domain and the dimer grows at the expense of the monomer domain. (b) Movie 2 shows a sequence of images demonstrating the formation of a few dimers within a monomer domain, followed by the expulsion of these dimer molecules. (c) Movie 3 demonstrates the quality of the images one typically obtains with our fast scanning tunneling microscope. The reduced image quality of movie 1 and movie 2 is due to the dynamics induced by illumination. Note that care was taken to avoid heating of the sample.

Ⓦ Movies Ⓦ 1, Ⓦ 2, and Ⓦ 3 are available in .avi format.

There are two possible dimers of **trans-C18CinnC18**, namely α-truxillic or β-truxinic derivatives (Scheme 1).[15] The location of the bright structures suggests that they correspond to the core of the dimer molecule, which consists of the two phenyl rings and a cyclobutane ring. For an α-truxillic derivative, the core of the dimer is expected to appear in the STM image as two distinctive bright circles lying on opposite sides of a dark line going through the

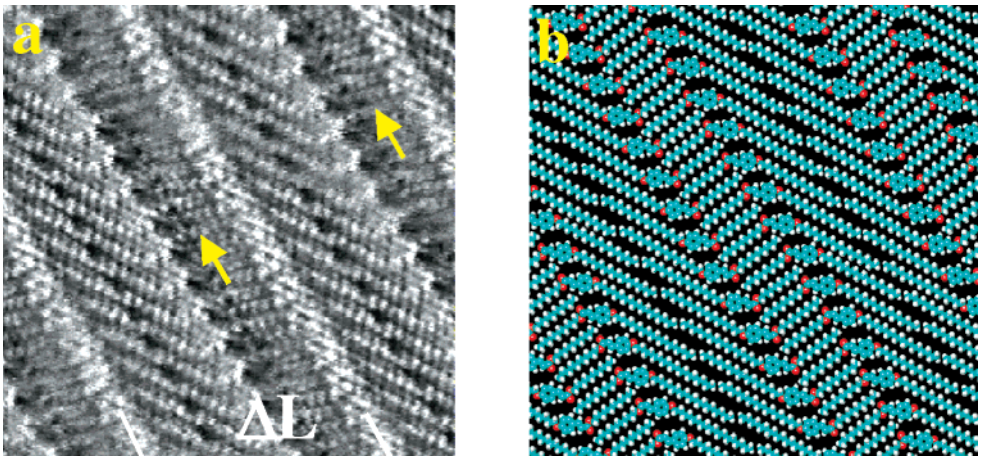

Figure 5. (a) STM image of **C18CinnC10**. Yellow arrows point to the C10 alkyl chains. The C10 alkyl chains are interdigitating. Image area is 11.3 × 11.3 nm^2, $V_{set} = -0.304$ V, $I_{set} = 1.0$ nA. (b) Molecular model of the monolayer shown in (a).

middle of the whole lamella. On the other hand, the β-truxinic derivative core is expected to appear as a U-shaped bright structure. In the STM image in Figure 3a, the bright structures in the center of a lamella appear to be U-shaped. Comparing this contrast with the structure of the two possible dimers (Scheme 1) suggests that the β-truxinic derivative is formed. A molecular model for the dimer molecule is proposed in Figure 3b. The packing parameters are $a = 24.0 \pm 0.5$ Å, $\Delta L = 61 \pm 4$ Å.

Because the STM images suggest the formation of the β-truxinic derivative, it must be **trans-C18CinnC18** domains of Type 1 orientation that lead to this derivative. Type 2 should produce the α-truxillic derivative, for which no evidence was found.

In addition to the experiments outlined above, the photodimerization of **C18CinnC18** at the graphite/liquid interface has been visualized at an increased scan rate using a fast scanning STM (2 frames per second), which allows for simultaneous recording on a videotape. A detailed description of the fast scanning STM system is given elsewhere.[6] In the experiments involving the modified STM, the samples were irradiated during scanning. A liquid light guide directs the light from a Xenon lamp, which is passed through heat filters and through a band-pass filter [UG5 Schott filter, 250−400 nm] to the graphite substrate. During imaging, care was taken that the same region of the monolayer was imaged during the recording time. The packing pattern of the adlayer of the dimer molecules is very distinctive from that of the monomer molecule adlayers, which allows the clear differentiation between the two adlayers. In a first sequence of images (Figure 4a and movie 1) obtained at a monomer/dimer domain boundary, the dimer molecules appear in a stepwise process. First, those monomer **C18CinnC18** molecules closest to the domain boundary shared with the newly formed dimer domain lose resolution due to enhanced mobility. This is followed by the appearance of dimer molecules at the same place that was previously occupied by the monomer molecules. In addition, photodimerization was observed in the bulk of the domain. In this case the dimer molecules were expelled from the adlayer, as the monomer adlayer cannot optimize the packing of the dimer molecules (Figure 4b, movie 2). Movie 3 (Figure 4c) demonstrates the quality of the image recording under illumination-free conditions.

To understand the effect of the 2D structure upon the photodimerization, **C18CinnC10** was investigated, as it was expected to bias Type 1 over Type 2 packing due to its asymmetric structure. Figure 5a shows an STM image of the monolayer of **C18CinnC10**. The monolayer structure is different from the one obtained for **C18CinnC18** (Figure 2). The decyl chains are clearly identified (indicated by yellow arrows) as being the shorter alkyl chains. They adopt a 90° angle with respect to the lamella axis as opposed to 40° for the octadecyl chain. Within a lamella, the **C18CinnC10** molecules have the decyl chains lying at the same side of the cinnamate group. The decyl chains are interdigitating, while octadecyl chains are not. Figure 5b shows the proposed molecular model of the observed monolayer: $a = 9.0 \pm 0.2$ Å, $\Delta L = 49.9 \pm 0.8$ Å. In contrast to **C18CinnC18**, **C18CinnC10** monolayers did not show any change upon irradiation. In addition, irradiation of concentrated solutions or solid crystals did not give any trace of dimer molecules.

According to the topochemical postulates and based upon the distances measured for both **C18CinnC18** and **C18CinnC10** monomer monolayers, neither of the two compounds was expected to photodimerize. Nevertheless, evidence provided by the STM experiments and the concentration dependent measurements strongly indicate that the photodimerization of **C18CinnC18** does take place within the monolayer. Two approaches were formulated to explain the reactivity of systems in 3D that, according to the topochemical postulates, should not react. Cohen formulated "the role of the reaction cavity", according to which the topochemical postulates can be refined to "reactions proceeding under lattice control do so with minimal change or distortion of the surface of the reaction cavity".[21−24] Gavezzotti has investigated the role of molecular environment in the crystal toward reactivity as well and has generalized that a prerequisite for crystal reactivity is the availability of free space around the reaction site.[25−27] In the second approach, Craig et al. pointed out the role of "dynamic preformation",

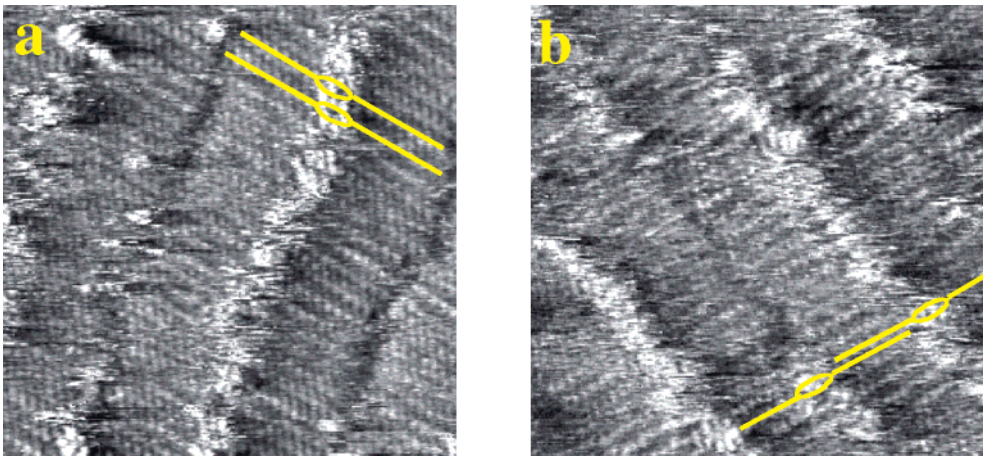

Figure 6. (a) STM image showing the extended conformation of **C18CinnC18** monomers. This kind of image is observed after short irradiation intervals in-situ. Two molecules are drawn schematically. Image area is 10.5 × 10.5 nm^2, $V_{set} = -0.73$ V, $I_{set} = 0.75$ nA. (b) STM image showing the extended conformation of **C18CinnC18** monomers. The image shows a part of the monolayer interdigitating (bottom right). Two molecules are drawn schematically. The image area is 10.1 × 10.1 nm^2, $V_{set} = -0.77$ V, $I_{set} = 0.6$ nA.

which might influence product formation.[28−31] Dynamical preformation can be summarized as follows: short-term lattice instability can have the effect of driving one molecule close to a neighbor so as to cause a photochemical reaction. This also can include rotation of the molecule into a more favorable orientation to allow the reaction to occur. Packing fluctuations are believed to be responsible for the photodimerization for a nonideal monomer packing (distance > 4.2 Å, nonparallel double bonds).

Some of the STM images, which were acquired after 5 min of irradiation at 300 nm, displayed a different packing pattern (Figure 6a) than those observed after longer irradiation periods. The image allows us to identify the alkyl chains and the cinnamate groups in the lamellae. There is a lot of distortion in the image, and, in certain parts of the image, the distortion does not always allow the identification of individual cinnamate groups. Such a distortion is usually associated with a loose packing of the molecules (packing fluctuations), which leads to an increased mobility of the molecules or parts thereof. Another indication of the high mobility of the molecules is the variation in the lamella width. More importantly, the images show that the conformation of the molecules is no longer V-shaped, instead the molecules appear to have adopted a linear conformation. The distance between adjacent molecules is found to be 3.9 ± 0.2 Å, thus the aryl moiety must be tilted out of plane in order to allow this packing pattern. This explains the loss of resolution in the image, especially for the cinnamate groups, as the tilting of the molecules out of plane reduces the packing efficiency and hence increases the mobility of the molecules in the monolayer.[8] This packing pattern also increases the overlap of the π-orbitals of the neighboring monomers, which is expected to facilitate dimerization. These observations emphasize the importance of packing fluctuations, where neighboring molecules have space to approach each other. Also, the loss of resolution in case of the fast scanning STM experiment followed by the appearance of the dimer molecules further points out the importance of packing fluctuations. However, a number of molecules are found to be interdigitating (Figure 6b). In this case the distance between successive molecules in the same lamella is found to be 8.5 ± 0.4 Å, hence the aryl moieties can remain parallel to the graphite plane. In Figure 6, two molecules are schematically indicated. In the case of **C18CinnC10**, the photostability can be explained as being due to interdigitation, leading to an increased intermolecular distance and hindering packing fluctuations.

In conclusion, the photodimerization of cinnamate derivatives monolayers at the graphite/liquid interface has been studied with STM. **C18CinnC18** molecules were found to pack in two patterns, Type 1 and Type 2. There was no difference in the packing parameters between the two types. **C18CinnC18** was not expected to dimerize according to the topochemical postulates. Nevertheless, STM provided evidence of photodimerization which was explained by means of packing fluctuations, allowing the reactive centers to approach each other. **C18CinnC10** was chosen in the hope to bias one of the two possible orientations of the monomer molecules over the other. Instead, these molecules were found to be interdigitated and resistant to photodimerization. In addition to the increased intermolecular distance, the interdigitation of the monomer molecules limits packing fluctuations. This further emphasizes the importance of the less closely packed adlayer structure of **C18CinnC18**.

Acknowledgment. The authors thank the DWTC, through IUAP-IV-11, and ESF SMARTON for financial support. S.D.F. thanks the Fund for Scientific Research − Flanders for financial support. The collaboration was made possible thanks to the TMR project SISITOMAS.

Supporting Information Available: Synthesis details of **C18CinnC18** and **C18CinnC10**. This material is available free of charge via the Internet at http://pubs.acs.org.

References

(1) McGonical, G. C.; Bernhardt, R. H.; Thomson, D. *J. Appl. Phys. Lett.* **1990**, *57*, 28.

(2) Rabe, J. P.; Buchholz, S. *Science* **1991**, *253*, 424.
(3) Frommer, J. *Angew. Chem., Int. Ed. Engl.* **1992**, *31*, 1298.
(4) Cyr, D. M.; Venkataraman, B.; Flynn, G. W. *Chem. Mater.* **1996**, 1600.
(5) De Feyter, S.; Gesquière, A.; Abdel-Mottaleb, M. M.; Grim, P. C. M.; Sieffert, M.; Meiners, C.; Valiyaveettil, S.; Müllen, K.; De Schryver, F. C. *Acc. Chem. Res.* **2000**, *33*, 520.
(6) Gesquière, A.; Abdel-Mottaleb, M. M.; De Feyter, S.; De Schryver, F. C.; Sieffert, M.; Mullen, K.; Calderone, A.; Lazzaroni, R.; Bredas, J. L. *Chem. Eur. J.* **2000**, *6*, 3739.
(7) Padowitz, D. F.; Messmore, B. W. *J. Phys. Chem. B* **2000**, *104*, 9943.
(8) Stabel, A.; Heinz, R.; Rabe, J. P.; Wegner, G.; De Schryver, F. C.; Corens, D.; Dehaen, W.; Süling, C. *J. Phys. Chem.* **1995**, *99*, 8690.
(9) Lopinski, G. P.; Wayner, D. D. M.; Wolkow, R. A. *Nature* **2000**, *406* (6), 48.
(10) Takami, T.; Ozaki, H.; Kasuga, M.; Tsuchiya, T.; Mazaki, Y.; Fukushi, D.; Ogawa, A.; Uda, M.; Aono, M. *Angew. Chem., Int. Ed. Engl.* **1998**, *36* (7), 2755.
(11) Heinz, R.; Stabel, A.; Rabe, J. P.; Wegner, G.; De Schryver, F. C.; Corens, D.; Dehaen, W.; Süling, C. *Angew. Chem., Int. Ed. Engl.* **1994**, *33*, 2080.
(12) Vanoppen, P.; Grim, P. C. M.; Rucker, M.; De Feyter, S.; Moessner, G.; Valiyaveettil, S.; Müllen, K.; De Schryver, F. C. *J. Phys. Chem.* **1996**, *100*, 19636.
(13) Grim, P. C. M.; De Feyter, S.; Gesquière, A.; Vanoppen, P.; Rucker, M.; Valiyaveettil, S.; Moessner, G.; Müllen, K.; De Schryver, F. C. *Angew. Chem., Int. Ed. Engl.* **1997**, *36*, 2601.
(14) Cohen, M. D.; Schmidt, G. M. J.; Sonntag, F. I. *J. Am. Chem. Soc.* **1964**, *86*, 2000.
(15) Schmidt, G. M. J. *J. Am. Chem. Soc.* **1964**, *86*, 4.
(16) Dilling, W. L. *Chem. Rev.* **1983**, *83*, 1.
(17) Hasegawa, M. *Chem. Rev.* **1983**, *83*, 507.
(18) Ramamurthy, V.; Venkatesan, K. *Chem. Rev.* **1987**, *87*, 433.
(19) In case of irradiation for time intervals longer than 1 h, the sample (a drop of the solution containing molecules of **C18CinnC18** applied to the graphite surface) was placed on a stand in a closed beaker with excess of solvent (1-octanol).
(20) Clypool, C. L.; Faglioni, F.; Goddard, W. A., III; Gray, H. B.; Lewis, N. S.; Marcus R. A. *J. Phys. Chem. B* **1997**, *101*, 5978.
(21) Cohen, M. D.; Klein, E.; Ludmer, Z.; Yakhot, V. *Chem. Phys.* **1974**, *5*, 15.
(22) Cohen, M. D.; Yakhot, V. *Chem. Phys.* **1974**, *5*, 27.
(23) Cohen, M. D. *Angew. Chem., Int. Ed. Engl.* **1975**, *14*, 381.
(24) Cohen, M. D. *Mol. Cryst. Liq. Cryst.* **1979**, *50*, 1.
(25) Gavezzotti, A. *Nouv. J. Chim. Soc.* **1982**, *6*, 443.
(26) Gavezzotti, A. *J. Am. Chem. Soc.* **1983**, *105*, 5220.
(27) Gavezzotti, A. *J. Am. Chem. Soc.* **1985**, *107*, 962.
(28) Carig, D. P.; Mallet, C. P. *Chem. Phys.* **1982**, *65*, 129
(29) Carig, D. P.; Lindsay, R. N.; Mallet, C. P. *Chem. Phys.* **1984**, *89*, 187.
(30) Collins, M. A.; Carig, D. P. *Chem. Phys.* **1981**, *54*, 305.
(31) Norris, K.; Gray, P.; Carig, D. P.; Mallet, C. P.; Markey, B. R. *Chem. Phys.* **1983**, *79*, 9.

NL010034K